JOURNAL OF GEOPHYSICAL RESEARCH, VOL. 105, NO. D11, PAGES 14,593–14,598, JUNE 16, 2000

Intensity of the second and third OH overtones of H_2O_2, HNO_3, and HO_2NO_2

Hui Zhang and Coleen M. Roehl

Division of Geological and Planetary Sciences, California Institute of Technology, Pasadena

Stanley P. Sander

Jet Propulsion Laboratory, California Institute of Technology, Pasadena

Paul O. Wennberg

Division of Geological and Planetary Sciences, and Program of Environmental Engineering
California Institute of Technology, Pasadena

Abstract. The $3\nu_{OH}$ and $4\nu_{OH}$ of H_2O_2, HNO_3, and HO_2NO_2 have been observed. The band strengths of $3\nu_{OH}$ are $(7.0 \pm 1.8) \times 10^{-20}$, $(2.9 \pm 0.7) \times 10^{-20}$, and $(3.8 \pm 1.1) \times 10^{-20}$ cm^2 molecules^{-1} cm^{-1} for H_2O_2, HNO_3, and HO_2NO_2, respectively. Those of $4\nu_{OH}$ are $(4.5 \pm 1.6) \times 10^{-21}$, $(2.8 \pm 1.0) \times 10^{-21}$, and $(3.0 \pm 1.8) \times 10^{-21}$ cm^2 molecules^{-1} cm^{-1} for H_2O_2, HNO_3, and HO_2NO_2, respectively. The uncertainty is for one standard deviation. Assuming excitation of these modes by solar absorption is dissociative for HO_2NO_2, these measurements confirm that this process will play a small role in the atmospheric photochemistry of the lower stratosphere.

1. Introduction

From the time it was first observed in the gas phase [*Niki et al.*, 1977], peroxynitric acid (HO_2NO_2) has been thought to be important to the chemistry of the terrestrial atmosphere. It is the current understanding that HO_2NO_2 is formed in the atmosphere exclusively by the recombination of hydroperoxyl radical and nitrogen dioxide:

(R1) $HO_2 + NO_2 + M \rightarrow HO_2NO_2 + M$

and is removed by reaction with hydroxyl radicals, via photodissociation:

(R2) $OH + HO_2NO_2 \rightarrow$ products

(R3a) $HO_2NO_2 + h\nu \rightarrow HO_2 + NO_2$

(R3b) $\rightarrow OH + NO_3$

and in the troposphere, by thermal decomposition:

(R-1) $HO_2NO_2 + M \rightarrow HO_2 + NO_2 + M$

Reaction (R-1) is unimportant above 7 km because of the low temperature and pressure [*Graham et al.*, 1977]. Assuming (R2) yields H_2O, O_2, and NO_2, the net result of (R1) and (R2) is to remove odd hydrogen radicals ($HO_x \equiv OH + HO_2$):

(R1+R2) $OH + HO_2 \rightarrow H_2O + O_2$

On the other hand, the photodissociation of HO_2NO_2 (reaction R3) produces a null cycle for HO_x. The importance of HO_2NO_2 as a HO_x sink is controlled by the rate of its formation (reaction R1) and by the ratio of the rates of (R2) to (R3).

Interest in the atmospherically important chemistry of HO_2NO_2 evolved from the realization that photochemical models, based on standard chemistry of the time, under estimated OH concentrations following sunrise, particularly in the lower stratosphere [*Wennberg et al.*, 1994; *Salawitch et al.*, 1994]. Since solar UV photons are strongly attenuated due to the long pathlength for ozone absorption at the large zenith angles at dawn, photochemical processes generating HO_x from light at visible wavelengths were proposed. *Donaldson et al.* [1997] presented calculations which indicated that excitation of OH overtone vibrations leading to dissociation in molecules such as HNO_3, HO_2NO_2, and H_2O_2 could potentially contribute to the production of HO_x in the lower stratosphere at high zenith angles. HO_2NO_2 was considered to more likely to enhance the HO_x production than HNO_3 or H_2O_2 because the energy of the second and third overtones of HO_2NO_2 lie above its photodissociation threshold, while for HNO_3 or H_2O_2, excitation to the fourth and fifth overtone, respectively, is required. Recent twilight observations [*Wennberg et al.*, 1999] led to the suggestion that the wavelength responsible for producing HO_x must be longer than 650 nm and again that HO_2NO_2 was put forward as the likely source.

The importance of OH overtone excitation in HO_2NO_2 came into question though when the integrated absorption intensity of the $3\nu_{OH}$ band measured by *Fono et al.* [1999] was found to be 5 times too weak to account for the missing HO_x source [*Wennberg et al.*, 1999]. In the Fono et al. work the $3\nu_{OH}$ band intensities of both HO_2NO_2 and HNO_3 were measured in concentrated sulfuric acid solutions, and the gas phase spectrum for HO_2NO_2 was obtained by linearly scaling the HO_2NO_2 solution spectrum according to the gas-solution behavior observed with HNO_3. A cautionary note was given that "because of solvent effects on the overtone intensities, the solution phase results should not be directly compared with gas phase values."

Paper number 2000JD900118.
0148-0227/00/2000JD900118$09.00

Reported here is the first observation of the $3\nu_{OH}$ and $4\nu_{OH}$ cross sections of HO_2NO_2 vapor between 700 and 1100 nm. Overtone intensities for HNO_3 and H_2O_2 were also obtained. On the basis of these measurements the importance of overtone-initiated photodissociation for the atmospheric chemistry of HO_2NO_2 is discussed.

2. Experiment

In this two-color direct absorption experiment, both the UV and near-IR absorbance are simultaneously measured in a flow tube. The recommended UV cross sections of H_2O_2, HNO_3, and HO_2NO_2 [*DeMore et al.*, 1997] are used to quantify the concentrations of these species. The measured near-IR optical depths can then be directly converted to absolute cross sections.

2.1. Instrumentation

The optical/vacuum apparatus used in this study has been described previously [*Watson et al.*, 1979]. The configuration used in this experiment is shown in Figure 1. The system is composed of two lamp sources, the absorption cell/vacuum system, and the UV and near-IR detectors.

Collimated light from a 250 W Quartz-tungsten-halogen lamp (Oriel, part 6334) and a deuterium lamp (Hamamatsu, model L1314X) are combined at dichroic mirror 1 (Oriel, part 66217), which reflects $260 < \lambda < 320$ nm and transmits $\lambda > 350$ nm. The beam is then folded by two 45° reflectors into a multipass absorption cell through a 4 mm aperture. Both the two reflectors and the White cell mirrors are MgF_2–coated aluminum.

The Pyrex absorption cell is 90 cm long and has an inner diameter of 30 mm. Light passes through it eight times. The cell has an outer cooling jacket where chilled methanol is circulated to maintain thermal control. Temperature is monitored with a thermocouple probe located at 7 cm from the end. Pressure in the cell is monitored with a thermocouple pressure gauge and a capacitance manometer (MKS Instruments). The absorption cell can be evacuated to less than 10 mtorr by a mechanical pump with a liquid nitrogen trap in line. Two 1-inch quartz windows are fused onto a quartz tube, which is sealed to the absorption cell with an O-ring joint. When the cell is cooled, the windows are purged from outside with dry nitrogen gas to prevent condensation. After eight passes, light exits the absorption cell, and then the UV and the visible/near-IR probe beams are separated at a second dichroic mirror that has the same spectral characteristics as dichroic mirror 1.

The UV light is focused into a 0.5 m UV monochromator (216.5 GCA/McPherson) equipped with a 2400 grooves/mm grating blazed at 240 nm. The light is detected by a multialkali photocathode photomultiplier tube (Hamamatsu R955) operated at ~750 V. Just before entering the monochromator, the UV beam is modulated at 2 kHz with an optical chopper (New Focus). The PMT current is processed by a lock-in amplifier (Stanford Research Systems). The widths of both the entrance and the exit slits on the monochromator are set at 500 μm. Scattered light is negligible for the UV system at the wavelength region used in this experiment. The monochromator wavelength scale is calibrated with a Hg lamp. This lamp is also used to confirm the spectral resolution of 0.3 nm.

The visible/near-IR light is dispersed with a 0.32 m monochromator (ISA, HR320) equipped with a 1024-element silicon photodiode array detector (EG&G, model 1412). A long-pass filter (Corion, LL700) is placed in the collimated beam to minimize the interference from the higher-order light. The 300 grooves/mm grating (blazed at 1.0 μm) combined with the entrance slit of 50 μm produces a spectral resolution

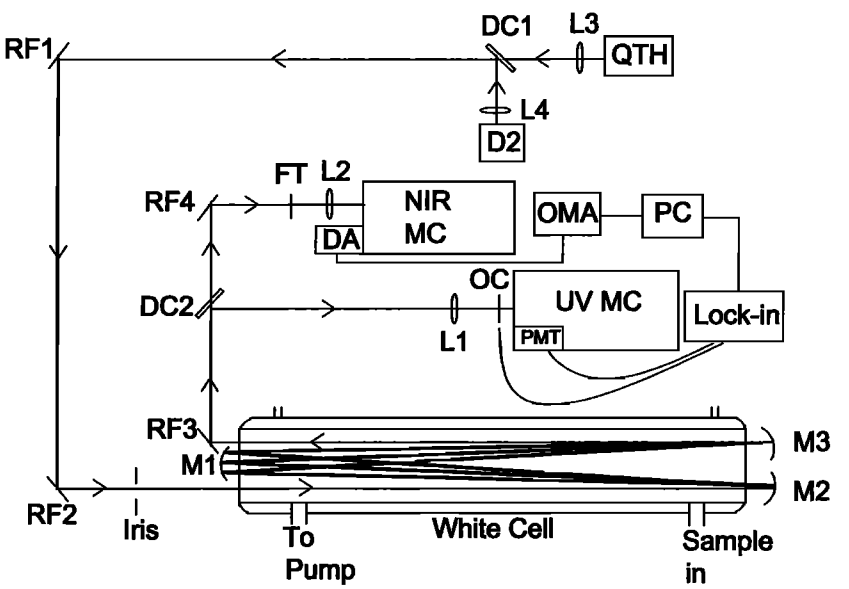

Figure 1. Schematic diagram of the two–color absorption experiment setup. D_2, deuterium lamp; DA, diode array detector; DC1, DC2, dichroic mirrors; FT, long-pass filter; L1, L2, focusing lenses; L3, L4, collimating lenses; M1, M2, M3, White Cell mirrors; NIR MC, near-IR monochromator; OC, optical chopper; OMA, optical multichannel analyzer; PMT, photon multiplier tube; QTH, quartz tungsten halogen lamp; RF1, RF2, RF3, RF4, reflectors; UV MC, UV monochromator.

of 0.5 nm (full width at half maximum (FWHM)). This performance is confirmed by recording the spectrum of a low-pressure Argon pen ray lamp.

The visible/near-IR absorption spectra were recorded in segments of about 250 nm, while the UV absorbance are monitored at a single wavelength. For comparison, measurements were made at both 250 nm and 260 nm. The smallest near-IR absorbance detectable is 2×10^{-4}. Besides noise in the electronics and lamp drift, an interference from water adsorbed to the cell windows limits the smallest UV detection to absorbance of $\sim 1 \times 10^{-2}$. In addition, scattered light in the White cell causes curvature in the Beer's law plot at optical depths as low as 3, and so all the data reported here were taken at lower optical depths.

2.2. HO_2NO_2 Synthesis

HO_2NO_2 was prepared in a nitrogen-purged glove box according to the method described by *Kenley et al.* [1981]. Briefly, ~1 g BF_4NO_2 (Aldrich, 95+%) was slowly added into ~5 mL of 95+ wt% H_2O_2 in ~50 mg increments. The highly concentrated H_2O_2 was obtained by distillation of 70 wt% H_2O_2 (FMC). The mixture was vigorously stirred in a jacketed glass vessel with water, cooled to ~273 K, circulating around it. Once the synthesis was finished, the mixture was quickly transferred to a glass bubbler, and then the bubbler was immediately immersed into an ice/water bath.

Impurities were always found in the prepared HO_2NO_2. Among them, HNO_3, H_2O_2, and NO_2 are problematic because they absorb at the UV wavelengths used to quantify $[HO_2NO_2]$. The strengths of $3\nu_{OH}$ for H_2O_2 (95+ wt%) and HNO_3 (Fisher, minimum 69.0%, maximum 71.0%, used without further purification) were determined in separate experiments using their known cross sections [*DeMore et al.*, 1997] at 250 nm and 260 nm. The spectrum of NO_2 over the visible/near-IR region was also measured. Throughout the experiment, the concentrations of these impurities were monitored using their distinct visible and near-IR absorption features in order to estimate their contributions to the observed UV absorption. The typical impurities levels are $[H_2O_2] \sim (6–7) \times 10^{15}$ cm^{-3}, $[HNO_3] < 4 \times 10^{14}$ cm^{-3}, and $[NO_2] \sim (1–1.5) \times 10^{14}$ cm^{-3}, and the typical $[HO_2NO_2]$ is in the range of $(2.5–10) \times 10^{15}$ cm^{-3}.

2.3. Spectra Acquisition and Analysis

All data were obtained by flowing argon (UHP/Zero Grade, Air Products) through a bubbler to carry the sample into the absorption cell. The glass sample bubbler was connected as closely as possible to the inlet of the absorption cell with only glass in between to avoid decomposition of the samples. HO_2NO_2 data were obtained with both the bubbler and the absorption cell kept at 273 ± 1 K and the carrier gas precooled by passing it through a copper coil emerged in ice-water mixture. Data for HNO_3 and H_2O_2 were obtained near room temperatures (297 ± 2 K). In addition, data for H_2O_2 at ~273 K were obtained to study the temperature dependence of its near-IR cross section.

Two flow configurations were used. For HNO_3 and H_2O_2 the argon flow over the sample was combined with a larger flow of pure argon as a means of varying the concentration of the analyte. In the case of HO_2NO_2 the concentration of HO_2NO_2 in the sample gradually decreased during the experiment, hence it was not necessary to vary the concentration by dilution. A solenoid control valve was employed to maintain a constant pressure (~35 torr) inside the cell between the background and the sample spectra.

The absorption spectra of HO_2NO_2 was recorded in the 700–1000 nm region and smoothed subsequently to a resolution of ~1 nm. We found that for some HO_2NO_2 samples the amount of HNO_3 and NO_2 was negligible. For others, however, HNO_3 and NO_2 were elevated initially, but after bubbling argon through the sample for 5–10 min, the concentration of HNO_3 and NO_2 was reduced significantly. This is illustrated in Figure 2 by two typical raw spectra taken from the same HO_2NO_2 sample. Identified on the spectra are

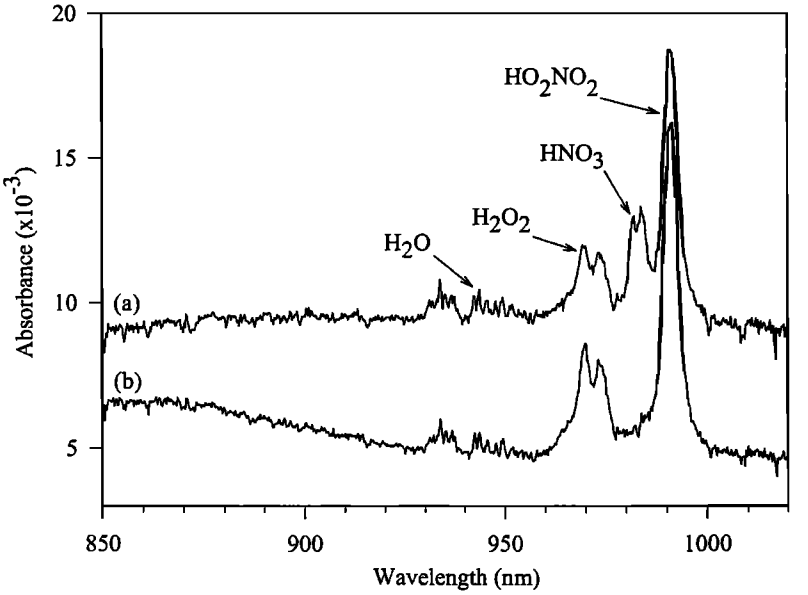

Figure 2. Raw spectra of HO_2NO_2. (curve a) Initial spectrum; (curve b) after about 5 min of flow, when HNO_3 impurity has been significantly reduced. The negative-going spikes may be due to the nonlinearity of the detector.

$3\nu_{OH}$ for HO_2NO_2, HNO_3, and H_2O_2, as well as H_2O. The grating was moved from time to time to the stronger NO_2 visible band [*Kirmse et al.*, 1997] to monitor its concentration. For the HO_2NO_2 data reported here, HNO_3 and NO_2 impurities contribute less than 0.2% of the total UV optical depth and thus are not considered further in the spectral analysis.

H_2O_2 was present as a significant impurity in all our HO_2NO_2 samples. In the analysis it is assumed that no species other than HO_2NO_2 and H_2O_2 contribute to the UV absorbance:

$$A_{UV,H2O2} + A_{UV,HNO4} = A_{total\ UV} \quad (1)$$

The contribution of H_2O_2 is subtracted from the UV absorbance using the ratio of the UV to overtone intensities determined in this study:

$$A_{UV,H2O2} = (\sigma_{UV,H2O2}/\sigma_{NIR,H2O2}) \times A_{NIR,H2O2} \quad (2)$$

The absolute intensity of the overtone of HO_2NO_2 is then calculated from the measured near-IR absorbance and its known UV cross section [*DeMore et al.*, 1997]:

$$\sigma_{NIR,HO2NO2} = (A_{NIR,HO2NO2}/A_{UV,HO2NO2}) \times \sigma_{UV,HO2NO2} \quad (3)$$

For the data reported here, only those measurements when HO_2NO_2 contributes more than 60% of the UV optical depth are used. The baseline fluctuation seen in Figure 2 is due to unknown origin. Corrections have been made to the baseline as part of the spectral processing.

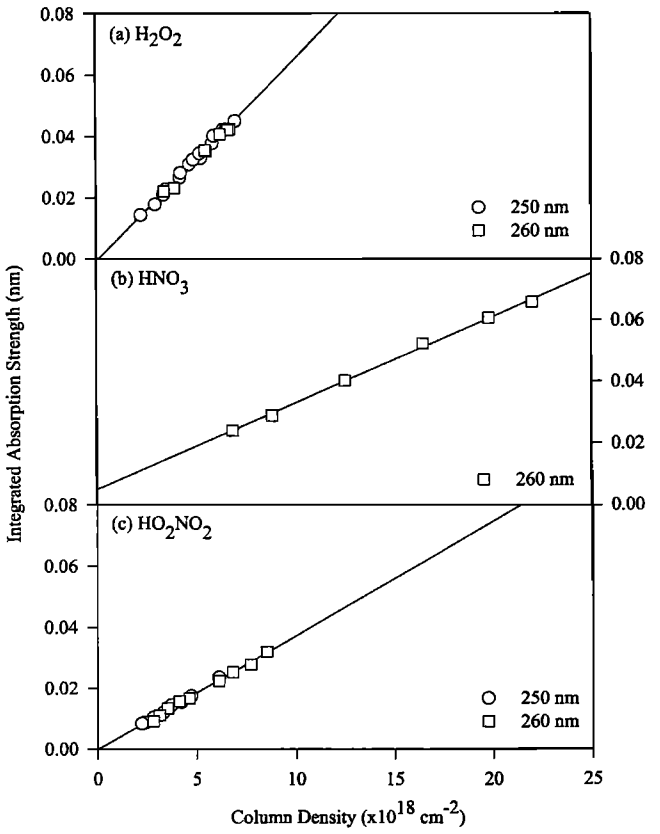

Figure 3. Plot of the band strength for $3\nu_{OH}$ as a function of column density derived from the absorbance measurements at 250 nm and/or 260 nm. (a) H_2O_2, including samples taken at both room temperature and ~273 K; (b) HNO_3; (c) HO_2NO_2 after accounting for H_2O_2.

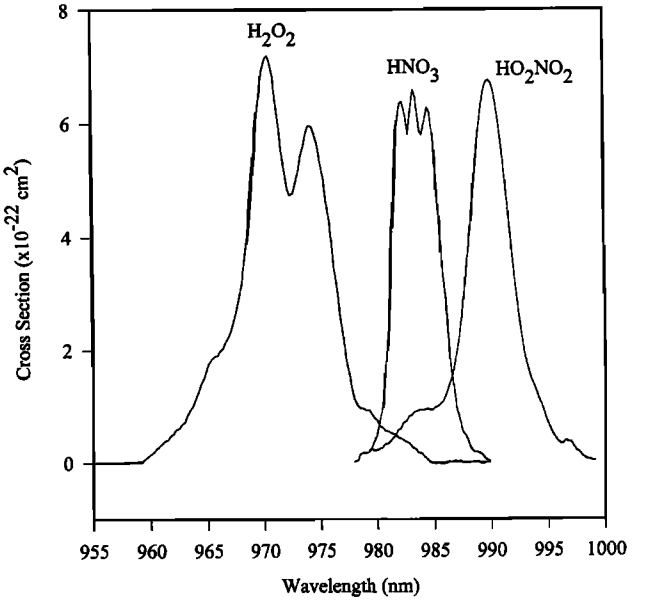

Figure 4. Spectrum of $3\nu_{OH}$ for H_2O_2, HNO_3, and HO_2NO_2 at a resolution of ~1 nm. They were taken at room temperature for H_2O_2 and HNO_3, and at ~273 K for HO_2NO_2.

3. Results and Discussion

3.1. Overtone Intensities

Shown in Figure 3 is the plot of the integrated optical depth of $3\nu_{OH}$ as a function of column density for H_2O_2, HNO_3, and HO_2NO_2. The slope of the least squares fit gives the integrated cross section. For H_2O_2, within the precision of these measurements, there is no temperature dependence of the IR cross section. The spectra of the $3\nu_{OH}$ for HNO_3, H_2O_2, and HO_2NO_2 are shown in Figure 4. Essentially the OH stretch is of similar strength in these three molecules. The $4\nu_{OH}$ of H_2O_2, HNO_3, and HO_2NO_2 are also observed. Table 1 summarizes the observed peak positions, the band strengths, and the oscillator strengths for these overtones.

The uncertainty in the reported cross section has two components: our experimental uncertainty and the uncertainty of the UV cross sections from previous studies. The former is mainly composed of the observed S/N (5% for $3\nu_{OH}$ and 15% for $4\nu_{OH}$), uncertainties in the baseline (10%), and, in the case of HO_2NO_2, error in our estimate of the contributions due to H_2O_2, NO_2, and HNO_3 (5%). On the basis of the original papers used in the JPL97 assessment [*DeMore et al.*, 1997], we estimate the uncertainty in the UV cross sections is 10% for all the three species at 250 nm and 260 nm.

The band strength for HNO_3 is in good agreement with the measurements of *Donaldson et al.* [1998]. The locations of the H_2O_2 bands agree with previous measurements [*Zumwalt and Giguere*, 1941; *Douketis and Reilly*, 1989]. For HO_2NO_2 the observed peak position for both $3\nu_{OH}$ and $4\nu_{OH}$ is in excellent agreement with the ab initio calculation of *Fono et al.* [1999]. The measured oscillator strength is within 25% for $3\nu_{OH}$ and 15% for $4\nu_{OH}$ of the same calculation. Interestingly, despite the puzzling fact that the solution spectrum of $3\nu_{OH}$ is blue-shifted by as much as ~20 nm for HO_2NO_2 while for HNO_3 it is red-shifted by ~32 nm, the relative intensity

Table 1. OH Overtones in H_2O_2, HNO_3, and HO_2NO_2

	Peak Position, nm			Band Strength, $x10^{-21}$ cm^2 molecules^{-1} cm^{-1}				Oscillator Strength, $x10^{-9}$		
	This Work	Ab Initio	Previous Work	A[a]	B[a]	C[a]	1σ,[b] %	This Work	Ab Initio	Previous Work
$3\nu_{OH}$										
H_2O_2	970	-	972[c]	70	69	70	15	79	-	-
HNO_3	983	-	983[d]	-	29	29	15	33	-	26.3[d]
HO_2NO_2	991	990[e]	-	40	38	38	20	43	56.6[e]	-
$4\nu_{OH}$										
H_2O_2	747	-	748[f]	4.3	4.5	4.5	25	5.0	-	-
HNO_3	755	-	755[d]	-	2.8	2.8	25	3.2	-	2.37[d]
HO_2NO_2	763	762[e]	-	-	-	3.0[g]	50	3.4	4.0[e]	-

[a]"A" is from UV measurements at 250 nm, "B" is from 260 nm, and "C" is to fit all the data points. UV cross sections used in data analysis from *DeMore et al.* [1997] in 10^{-20} cm^2 molecules^{-1} are as follows: at 250 nm, 298 K, 8.3, 1.97, and 41.2 for σ_{H2O2}, σ_{HNO3}, and σ_{HO2NO2}, respectively; at 250 nm, 273 K, 8.3, 1.91, and 41.2 for σ_{H2O2}, σ_{HNO3}, and σ_{HO2NO2}, respectively; at 260 nm, 298 K, 5.3, 1.91, and 28.5 for σ_{H2O2}, σ_{HNO3}, and σ_{HO2NO2}, respectively; at 260 nm, 273 K, 5.2, 1.86, and 28.5 for σ_{H2O2}, σ_{HNO3}, and σ_{HO2NO2}, respectively. On the basis of the original papers for the JPL assessment we estimate the uncertainty (1σ) is 10% for the UV cross sections.
[b]One standard deviation not including uncertainty in the UV cross sections.
[c]From *Zumwalt and Giguere* [1941].
[d]From *Donaldson et al.* [1998].
[e]From *Fono et al.* [1999]. See text for details.
[f]From *Douketis and Reilly* [1989].
[g]Estimation based on only two measurements.

scaling between gas and solution spectrum predicts gas-phase HO_2NO_2 cross sections in good agreement with our measurements.

3.2. Atmospheric Significance

Excitation of $3\nu_{OH}$ and $4\nu_{OH}$ will play a small role in the atmospheric photochemistry of HO_2NO_2 provided that this process is dissociative. The solar flux near 10,000 cm^{-1} (i.e., 1000 nm) is approximately 4×10^{13} photons cm^{-2} s^{-1} cm^{-1} [*Neckel and Labs*, 1984]. Because the atmosphere is essentially transparent at this wavelength, the actinic flux is approximately the same as the solar flux and will not vary with solar zenith angle (SZA) during the daytime (neglecting the planetary albedo). Thus, by simply multiplying our measured integrated band strength by the solar flux, we obtain a photolysis rate for HO_2NO_2 via excitation of $3\nu_{OH}$ of $\sim 1.5 \times 10^{-6}$ s^{-1}, essentially independent of SZA. Photolysis of HO_2NO_2 in the UV, on the other hand, depends strongly on the ozone optical depth and thus drops off rapidly with increasing SZA. Excitation of $3\nu_{OH}$ significantly increases the photolysis rate of HO_2NO_2 in the lower stratosphere only for SZA > 80° (R. J. Salawitch, personal communication, 1999). Therefore, only at high latitudes, where the Sun remains at high SZA for a significant fraction of the day, will inclusion of this overtone-induced dissociation process alter the calculated concentration of HO_2NO_2 [*Wennberg et al.*, 1999]. For equinox conditions at 60° latitude the overtone excitation increases the 24-hour average photolysis rate of HO_2NO_2 by approximately 20% in the lower stratosphere. At lower latitudes the increase is much smaller (a few percent).

Wennberg et al. [1999] calculated that a SZA-independent HO_x source of approximately 3×10^3 molecules cm^{-3} s^{-1} was missing from photochemical models during daylight. If photolysis of HO_2NO_2 in the near-IR is responsible, a rate of 1.2×10^{-5} s^{-1} is required to match this source. Assuming the dissociation quantum yield is unity, this is nearly an order of magnitude larger than can be contributed by the overtone excitation as determined in this study. *Wennberg et al.* [1999] suggested that in addition to $3\nu_{OH}$, excitation of combination bands of $2\nu_{OH}$ or broadband absorption to a low-lying triplet state of HO_2NO_2 might be responsible for the HO_x production. In this study we are unable to investigate these mechanisms because (1) the silicon diode array is not sensitive beyond 1100 nm (where the combinations bands would occur) and (2) the stability of the background is not sufficient to observe broadband weak absorption features (see Figure 2).

Acknowledgments. This work is partly supported by NASA grant SA98-0055. We thank R. J. Salawitch for help on the HO_2NO_2 photolysis rate calculations. Useful communications with D. J. Donaldson are greatly appreciated.

References

DeMore, W. B., S. P. Sander, D. M. Golden, R. F. Hampson, M. J. Kurylo, C. J. Howard, A. R. Ravishankara, C. E. Kolb, and M. J. Molina, Chemical kinetics and photochemical data for use in stratospheric modeling, *JPL Publ., 97-4*, 1997.

Donaldson, D. J., G. J. Frost, K. H. Rosenlof, A. F. Tuck, and V. Vaida, Atmospheric radical production by excitation of vibrational overtones via absorption of visible light, *Geophys. Res. Lett., 24*, 2651-2654, 1997.

Donaldson, D. J., J. J. Orlando, S. Amann, G. S. Tyndall, R. J. Proos, B. R. Henry, and V. Vaida, Absolute intensities of nitric acid overtones, *J. Phys. Chem. A, 102*, 5171-5174, 1998.

Douketis, C., and J. P. Reilly, High resolution vibrational overtone spectroscopy of hydrogen peroxide in the Δv=4 region, *J. Chem. Phys., 91*, 5239-5250, 1989.

Fono, L., D. J. Donaldson, R. J. Proos, and B. R. Henry, OH overtone spectra and intensities of pernitric acid, *Chem. Phys. Lett., 311*, 131-138, 1999.

Graham, R. A., A. M. Winer, and J. N. Pitts Jr., Temperature dependence of the unimolecular decomposition of pernitric acid and its atmospheric implications, *Chem. Phys. Lett., 51*, 215-220, 1977.

Kenley, R. A., P. L. Trevor, and B. Y. Lan, Preparation and thermal decomposition of pernitric acid ($HOONO_2$) in aqueous media, *J. Am. Chem. Soc.*, *103*, 2206–2220, 1981.

Kirmse, B., A. Delon, and R. Jost, NO_2 absorption cross section and its temperature dependence, *J. Geophys. Res.*, *102*, 16,089-16,098, 1997.

Neckel, H., and D. Labs, The solar radiation between 3300-A and 12500-A, *Solar Phys.*, *90*, 205-258, 1984.

Niki, H., P. D. Maker, C. M. Savage, and L. P. Breitenbach, Fourier transform IR spectroscopy observation of pernitric acid formed via HOO + $NO_2 \rightarrow HOONO_2$, *Chem. Phys. Lett.*, *45*, 564-566, 1977.

Salawitch, R. J., S. C. Wofsy, P. O. Wennberg, R. C. Cohen, J. G. Anderson, D. W. Fahey, R. S. Gao, E. R. Keim, E. L. Woodbridge, R. M. Stimpfle, J. P. Koplow, D. W. Kohn, C. R. Webster, R. D. May, L. Pfister, E. W. Gottlieb, H. A. Michelsen, G. K. Yue, J. C. Wilson, C. A. Brock, H. H. Jonsson, J. E. Dye, D. Baumgardner, M. H. Proffitt, M. Loewenstein, J. R. Podolske, J. W. Elkins, G. S. Dutton, E. J. Hintsa, A. E. Dessler, E. M. Weinstock, K. K. Kelly, K. A. Boering, B. C. Daube, K. R. Chan, and S. W. Bowen, The distribution of hydrogen, nitrogen, and chlorine radicals in the lower stratosphere: Implications for changes in O_3 due to emission of NO_y from supersonic aircraft, *Geophys. Res. Lett.*, *21*, 2547-2550, 1994.

Singer, R. J., J. N. Crowley, J. P. Burrows, W. Schneider, and G. K. Moortgat, Measurement of the absorption cross-section of peroynitric acid between 210 and 330 nm in the range 253–298 K, *J. Photochem. Photobiol. A Chemistry*, *48*, 17–32, 1989.

Watson, R. T., S. P. Sander, and Y. L. Yung, Pressure and temperature dependence kinetics study of the NO + BrO -> NO_2 + Br reaction: Implications for stratospheric bromine photochemistry, *J. Phys. Chem.*, *83*, 2936-2944, 1979.

Wennberg, P. O., R. C. Cohen, R. M. Stimpfle, J. P. Koplow, J. G. Anderson, R. J. Salawitch, D. W. Fahey, E. L. Woodbridge, E. R. Keim, R. S. Gao, C. R. Webster, R. D. May, D. W. Toohey, L. M. Avallone, M. H. Proffitt, M. Loewenstein, J. R. Podolske, K. R. Chan, and S. C. Wofsy, Removal of stratospheric O_3 by radicals: In situ measurements of OH, HO_2, NO, NO_2, ClO, and BrO, *Science*, *266*, 398-404, 1994.

Wennberg, P. O., R. J. Salawitch, D. J. Donaldson, T. F. Hanisco, E. J. Lanzendorf, K. K. Perkins, S. A. Lloyd, V. Vaida, R. S. Gao, E. J. Hinsta, R. C. Cohen, W. H. Swartz, T. L. Kusterer, and D. E. Anderson, Twilight observations suggest unknown sources of HO_x, *Geophys. Res. Lett.*, *26*, 1373-1376, 1999.

Zumwalt, L. R., and P. A. Giguere, The infra-red bands of hydrogen peroxide at λ9720 and the structure and torsional oscillation of hydrogen peroxide, *J. Chem. Phys.*, *9*, 458-462, 1941.

C. M. Roehl and H. Zhang, Division of Geological and Planetary Sciences, M/S 150-21, California Institute of Technology, Pasadena, CA 91125. (coleen@gps.caltech.edu; hui@gps.caltech.edu)

S. P. Sander, Jet Propulsion Laboratory, California Institute of Technology, Pasadena, CA 91109. (ssander@jpl.nasa.gov)

P. O. Wennberg, Division of Geological and Planetary Sciences, and Program of Environmental Engineering, M/S 150-21, California Institute of Technology, Pasadena, CA 91125. (wennberg@gps.caltech.edu)

(Received November 23, 1999; revised February 9, 2000; accepted February 11, 2000.)